

Metrological analysis of a procedure for the automatic 3D modeling of dental plaster casts

Nicola Brusco

Dept. of Information Engineer

University of Padova

nicola.brusco@dei.unipd.it

Simone Carmignato

DIMEG

University of Padova

simone.carmignato@unipd.it

Marco Andreetto

Dept. of Information Engineer

University of Padova

marco.andreetto@dei.unipd.it

Guido M. Cortelazzo

Dept. of Information Engineer

University of Padova

corte@dei.unipd.it

Abstract

As well known, in the reconstruction of the 3D models through optical systems, the errors are due to the single-view acquisition error and to the 3D modeling procedure. The latter can be ascribed to the various phases of the 3D modeling pipeline: pairwise registration, global registration, surface integration.

This work examines the acquisition error as well as the errors due to an automatic procedure recently proposed for the 3D modeling of dental plaster casts. This contribution derives a simple error propagation model, rather useful for practical simulation purposes.

From a general viewpoint, this contribution proposes a useful simulation of error propagation in 3D modeling, it shows the quality of an automatic 3D modeling procedure recently proposed and it shows the accuracy of 3D modeling dental plaster casts by current commercial range cameras and the considered automatic method.

1. Introduction

This work reports some preliminary results about a feasibility study aimed at the creation of a virtual gypsotheque of dental plaster casts initiated in cooperation with the Dental Clinic of the University of Padova. Since dental casts are freeform surfaces, such a project is an intriguing mixture of open issues concerning 3D modeling, geometrical metrology and medicine. With respect to 3D modeling it is necessary to devise automatic 3D modeling procedures suitable to be reliably performed by non-engineering personnel. With respect to metrology it is necessary to establish what accuracy the 3D models of dental casts and their possible physical duplicates need in order to be of clinical interest. The medical implications concern the best use of the mathematical information offered by the models.

An automatic 3D modeling procedure suited to this application was presented in [1]. This work concentrates on accuracy aspects and analyzes the errors of the 3D models obtained by such a procedure with a commercial range camera based on patterns projection as acquisition device.

This paper focuses on the results obtained on dental plaster casts; however, the technique can be extended to any kind of free-form surface.

Performance verification of measuring systems for complex measurements of free-form surfaces such as dental plaster casts is an intrinsically delicate task. Moreover, international standards on performance verification of optical systems are still missing. As a consequence, specifications provided by optical systems manufacturers on the accuracy of common commercial 3D systems are often not clearly interpretable: the parameters with which such specifications are expressed and the way in which they are determined differ from a producer to another. This increases the difficulties that are met by users to understand the accuracy of the 3D models obtained from optical systems. Because of the complexity of 3D optical measuring systems and their use in a large variety of applications, the assessment of measuring uncertainty for any possible measurement task is an extremely difficult issue. Therefore, a better approach is to evaluate the measuring uncertainty for individual measurement tasks. According to this approach, the result of a performance assessment is valid only for measurement tasks performed on similar objects and under similar measurement conditions. In this paper the method used for the assessment of the measurement performance of the 3D optical system is the well-known substitution method, in which repeated measurements are carried out on a calibrated object and measurement results are compared with the calibration data. This method can be used to evaluate the accuracy of geometrical measurements for virtually any measurement task [2] including the measurement of freeform surfaces [3]. In the work here presented, a CMM was selected as a more

accurate measuring system, providing the calibration data needed for comparison. CMMs are nowadays well accepted as the reference tool in industry for traceable 3D geometrical measurements [4].

The errors of the 3D models obtained by the automatic 3D modeling procedure of [1] (i.e., the distances between the points of the 3D model and the true points of the physical object) are due to the 1) acquisition error present in the single 3D views 2) the error in the automatic registration of pairs of 3D views 3) the error due to the ICP-based global alignment over all the 3D views 4) the error due to the fusion procedure, i.e., to the procedure returning a single surface from the set of registered clouds of points, each one associated to a 3D view. It is important to observe that while error source 1), i.e., the acquisition error, depends on the acquisition instrument, environmental conditions, operator and workpiece, error sources 2)-4) solely depend on the 3D modeling procedure.

We are especially interested to characterize error sources 2)-4) which qualify the 3D modeling procedure by [1] both because such a procedure could be modified if needed and because the acquisition error can be improved by deploying range cameras of higher performance/cost.

For this reason we will first examine the effect of error sources 1), acquiring the objects in different conditions; then we examine the cumulative effects of the various error sources of the modeling procedure, in order to be able to compare these data with those obtained by an error model decoupling the impact of error sources 2)-4) from the acquisition or single view error 1). We will show that there is a remarkable match between experimental and simulation data.

It will be seen that in light of the error contribution of the 3D modeling procedure of [1], if such a procedure is used with range cameras of appropriate performance one can obtain 3D models of considerable precision.

This paper is organized as follows: Section 2 recalls the 3D modeling procedure of [1] for reader's convenience. Section 3 examines the acquisition error introduced by single view acquisition. Section 4.1 analyzes the error due to registration and surface integration. Section 4.2 shows how the experimental data can be simulated by a simple analytical model. Section 5 draws the final remarks.

2. An automatic 3D modeling procedure

For clarity's sake, it will be useful to quickly recall the automatic 3D modeling method of [1]. The first two steps of the 3D modeling pipeline [5] traditionally concern the registration of all the 3D scans of an object, namely the mutual registration of all the pairs of 3D views, called pairwise registration, and the subsequent registration of all the 3D views, called global registration. The registration of a pair of partially overlapping 3D views is accomplished in two steps: a rough detection of the common region and a fine

estimate of the rigid rotation and translation (\mathbf{R}, \mathbf{t}) bringing the two 3D views to the best possible overlap (over the common region).

There exist two fundamental approaches to the automatic detection of a rough common region between a pair of partially overlapping 3D views. One rests on the use of invariant statistics for each point of the mesh [6] [7] [8] [9] [10] [11] [12], the other on the use of special features based either on geometry [13] [14] [15] [16], or on texture [17]. In principle the latter approaches can be more efficient, but less robust (for certain types of objects the wanted features may be missing or not easy to find). All methods, expectedly, have difficulties with highly symmetric objects or parts.

For the automatic detection of the common region we used the method of the spin-images of [12] [11], where the reader is referred to for a detailed presentation.

The final estimate of the rotation and translation (\mathbf{R}, \mathbf{t}) between two 3D views is typically accomplished by the ICP algorithm [18] or by some of its many variants. The rough prealignment obtained by way of spin-images is often adequate to bring the ICP to convergence. However this was not found to be always the case, consistently with the fact that the ICP algorithm is known to be able to produce very precise estimates of \mathbf{R} and \mathbf{t} when properly started. Otherwise it may be trapped by local minima. This problem may be overcome by initiating the ICP from different starting points, several strategies for their selection are proposed in the literature [19]. In practice this issue is commonly solved by manually selecting a few corresponding points from which an estimate of (\mathbf{R}, \mathbf{t}) is determined by Horn's algorithm.

In order to have a fully automatic procedure we use instead the frequency domain method of [20] as a robust device for determining a first estimate of the (\mathbf{R}, \mathbf{t}) parameters to use as starting point for the ICP. The frequency domain algorithm of [20] does not operate on a point-to-point correspondence logic as the ICP, since the Fourier transform makes a synthesis of all the available spatial information. The method of [20] and the ICP operate on very different principles and their combination turns out remarkably robust.

Since the frequency domain method does not operate directly on the 3D surface data, but it has to turn them into small volumes, it is not as precise as the ICP.

Global registration among all the 3D views is obtained by the method of [21] and surface integration from the registered views by the method of [22].

3. Acquisition error

We first verified the manufacturer's specs of our acquisition instrument by comparing the 3D views of the plaster casts obtained by our optical range camera against measurement obtained by a tactile probing Coordinate Measuring Machine (CMM). CMM acquires a certain number of points (1646 points, in this case) on the surface. A complete CAD

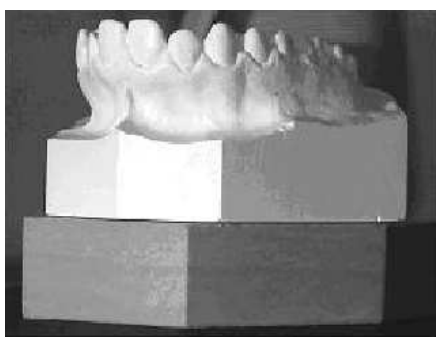


Figure 1. Reference block glued underneath a plaster cast.

	without repositioning	with repositioning
Average (mm)	0,0006	0,0009
St.Dev. σ (mm)	0,0339	0,0343

Table 1. Error for the acquisition of a single 3D view, with and without repositioning.

model of the surface is generated; this CAD model is verified for accuracy by checking a certain number of points on it (1861 points, in this case) with the CMM. A Maximum Permissible Error (MPE) is computed [23]. The CMM used for comparison has a MPE of $2.2 + L/300 \mu m$ (L in mm). In order to correct the probing errors, the CMM equipment needs to know the normal direction to each sensed point. For this reason, the CMM is not suited for accurately measuring complex free-form surfaces of which CAD models are not available, as in the case of dental casts. Therefore, instead of using the CMM to calibrate the geometry of a plaster cast, we measured a reference object with regular geometry: the prismatic solid underneath the plaster casts which is shown in Fig. 1.

The surface characteristics and dimensions of the chosen reference object are similar to the ones of the plaster casts to be measured. The reference object was measured by the CMM and a highly accurate CAD model of it was obtained.

The comparison between CAD model of the reference block and the data obtained by our optical range camera was obtained by a commercial parametric modeler [24].

In order to assess the single view measurements by the optical range camera, the same view was aquired N times ($N=10$), first without moving the reference block and then by repositioning the reference block before every acquisition (as typical of practical acquisition sessions). Table 1 summarizes the results in terms of mean and standard deviation. As Table 1 shows, repositioning implies a slight increase in σ .

Different views of the block were then acquired. The results are shown in Fig. 2 and Table 2. It can be seen that

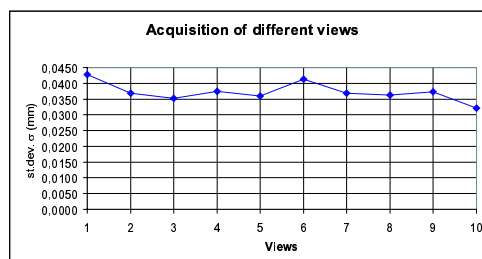
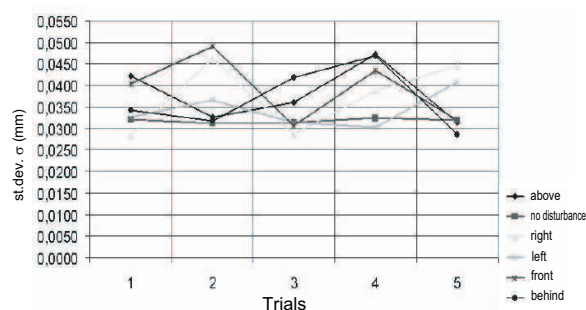


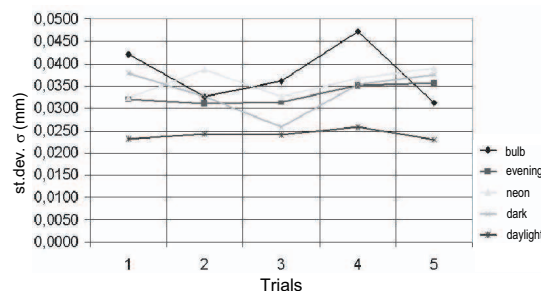
Figure 2. Error for the acquisition of different views.

Average (mm)	-0,0010
St.Dev. σ (mm)	0,0374

Table 2. Error for the acquisition of different views (each one averaged over 10 measurements).



(a) light's position



(b) illumination's type

Figure 3. Error a) under different light's positions; b) under different types of illumination

they do not differ significantly from those of Table 1.

We also examined the influence of a disturbance light in different positions and of the illumination's type. Fig. 3a) shows the standard deviation of 10 repeated acquisitions of the same 3D view with a disturbance illumination source placed in different positions (no disturbance means that the disturbance illumination is not present); Fig. 3b) shows similar data for different of illumination's types. The best

Volume of measure	100x100x75 mm
XY spatial resolution	0,13 mm
Z spatial resolution	0,010 - 0,020 mm
St.Dev. XY (σ)	0,05 mm
St.Dev. Z (σ)	0,045 mm

Table 3. Manufacturer's specification of the deployed optical range camera.

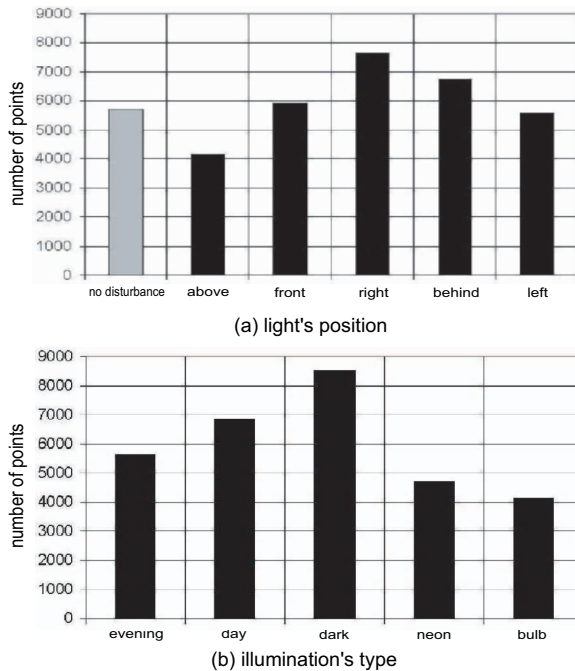


Figure 4. Number of measured points a) under different light's positions b) under different types of illumination

results are associated to day light since the optical range camera was calibrated under similar (diffuse) illumination's conditions.

It is also worth observing, from Fig. 4, that also the number of the actually acquired object's points is considerably influenced by the presence of a disturbance light and illumination's type. For instance, the highest number of points is acquired in presence of a disturbance light at the right (Fig. 4) and when no light illuminates the object (dark case in Fig. 4b)). However, under such conditions the points are also very noisy because the instrument was calibrated in a different situation and the overall quality of the measurement turns out worst than with other illumination's types. The best results are obtained, as expected, in the absence of an interfering light and under daylight diffuse illumination conditions.

Fig. 5 shows the results concerning the measurements of the same view under progressively degraded calibration set-

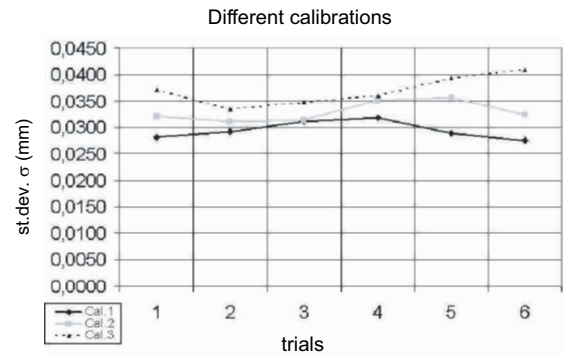


Figure 5. Error with respect to calibration setup.

ups. Namely, Cal1 is the correct calibration set-up, Cal2 is a slight modification of Cal1 and Cal3 is a further modification. These data show the relevance of proper calibration in order to get the best measurement performance.

The tests on the single view acquisition verified that our commercial optical range camera operates well within the manufacturers specifications shown in Table 3.

So far, we have not used the plaster cast yet but only the reference block.

4. 3D modeling error

4.1. Experimental assessment

As reminded in Section 2, pairwise registration in the 3D modeling procedure of [1] is performed in two steps, namely a coarse step obtained by means of spin-images and a fine step obtained by the ICP started via [20].

The automatic 3D modeling procedure of [1] which is able to model a dental plaster cast is not suited to model the reference block because of its piece-wise planar characteristics and because of its symmetries (it may be worth noting that these characteristics are the ones which enable the measurement by the CMM). In order to compare the accuracy of a 3D model obtained by our procedure with the CMM measurements we glued the reference object underneath the plaster casts, as shown in Fig. 1. By taking views of the "augmented" plaster cast including portions of both cast and reference object we are able to deploy our automatic 3D modeling procedure for its model. Indeed in this case spin-images are able to operate, since they can lock onto the irregular shape of the cast. Clearly the plaster cast "augmented" with the reference block is an object larger than the plaster cast itself and its 3D model requires a number of views larger than the number of views strictly necessary to model the plaster cast alone, namely 11 views vs. 6. Therefore the global modeling error on the augmented plaster cast will bound from above the error of the plaster cast alone. Furthermore for the accuracy's measurements we will compare only the portion of the 3D model concerning the reference object with its CMM based model.

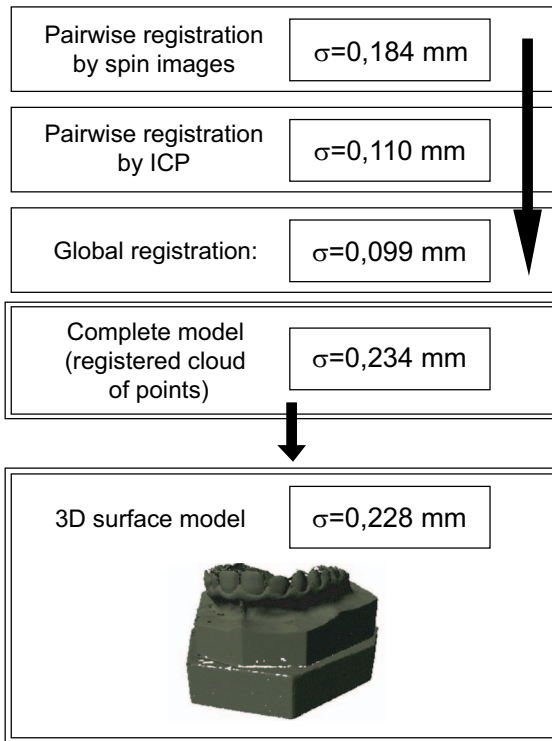


Figure 6. 3D modeling procedure and registration error in terms of experimentally determined σ .

Fig. 6 synthetically tracks the results of the 3D modeling error from pairwise registration, to global registration and surface integration.

More specifically the first three single frame blocks of the diagram of Fig. 7 refer to the accuracy of corresponding points on two different views after the various registration steps (i.e., conceptually, the point of view A and view B registered one over the other, which are associated to the same physical point of the object). The distances between corresponding points are only measured on the common region between pairs of registered views. More specifically, if A and B denote the sets of points of view A and view B registered one over the other, the common region is set $A^1 \cup B^1$, where $A^1 = A - (A - B)$ and $B^1 = B - (B - A)$. Let's recall that relatively to sets X and Z, set difference is defined as $X - Z = X \cap Z^c$, with Z^c complement of Z.

As shown in Fig. 6 the coarse pairwise registration by way of spin images leads to an error between corresponding points on the common region of mean $m = 0.0090mm$ and $\sigma = 0.184mm$, the fine pairwise registration by the ICP algorithm to an error of mean $m = -0.044mm$ and $\sigma = 0.114mm$. Pairwise registration is followed by global registration by the method of [21]. Such a global refinement further reduces the pairwise registration error between corresponding points on the common region to mean $m = 0,0035mm$ and standard deviation $\sigma = 0.099mm$.

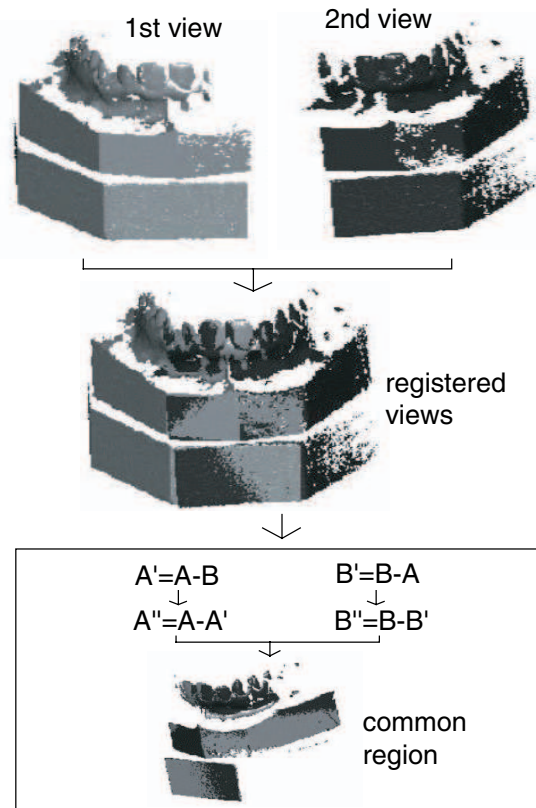


Figure 7. Common region between two registered views.

By considering only the portion of the augmented dental plaster cast concerning the reference object, we are able to measure the distances between the points positions on the 3D model and the points position on the CMM-based CAD model. The accuracy of such measurements is indicated by a double frame in Fig. 6.

It can be seen that the registration error considered over all the views and measured comparing only the portion part of the 3D model of the augmented dental plaster cast with respect to it CMM-based CAD model as Fig. 8 indicates has $m = 0.0426mm$ and $\sigma = 0.234mm$.

Surface integration reduces data redundancy of overlapped clouds of points by returning a mesh of triangles which "averages" them. We used the technique of [22] for 3D modeling the augmented plaster casts made by 11 3D views, at 3 different spatial resolutions, namely 64, 128 and 256 voxels. Table 4 shows that as the voxels number varies the average error remains between the $0.01mm$ and $0.02mm$, while standard deviation σ decreases from $0.2846mm$ down to $0.2283mm$ as the voxels number increases.

We also verified the impact of the number of used 3D views on the modeling error, by building a 3D model of

Voxels	64	128	256
Number of triangles	17565	91067	402003
Memory (Kb)	625	3567	16392
Measured points	1563	7019	29812
Volume (mm^3)	350642	359067	363155
Average error (mm)	-0.0097	-0.0021	-0.0175
Standard dev. σ	0.2846	0.2537	0.2283
Interval with 95% of the errors	-0.5757	-0.6236	-0.4812
Computation Time (sec)	275	387	724

Table 4. Parameters of augmented dental cast built from 11 3D views.

Voxels	64	128	256
Number of triangles	19143	83071	367545
Memory (Kb)	719	3115	14389
Measured points	1574	6910	29022
Volume (mm^3)	344191	355956	363155
Average error (mm)	0.0503	-0.0296	0.0075
Standard dev. σ	0.3130	0.2863	0.2468
Interval with 95% of the errors	-0.5982	-0.5736	-0.5346
Computation Time (sec)	498	624	1032

Table 5. Parameters of augmented dental cast built from 18 3D views.

an augmented dental plaster cast from 18 3D views, rather than from 11 3D views. Table 5 shows that the standard deviations of the 18 views 3D model are greater than those of the 11 views 3D models (and the computing times are obviously increased). The results of Table 4 and Table 5 indicate that for precision's purposes it is preferable to build 3D models with the smallest number of 3D views and with the highest voxel's resolution. One could expect that more views increase the accuracy, since acquisitions are averaged by integration. However the registration procedure introduces an error which accumulates as the number of views increases. Indeed, the error in a model made from 18 views is greater than the error in a model made from 11 views.

Therefore surface integration by means of [22], as expected, does not introduce any error since it smooths out the point-wise discontinuities of the overlapped clouds of points. Indeed the accuracy of errors between the CMM-based CAD model of the reference block and the 3D model's portion concerning it, remains essentially unchanged at $\sigma = 0.228mm$.

It is finally worth recalling that the final 3D modeling results reported above are plagued by the single view or acquisition error dependent on the acquisition instrument and refer to the 11 views of the 3D model of the plaster cast mounted above the reference block (let us again remind that only 6 views suffice to model the plaster cast alone).

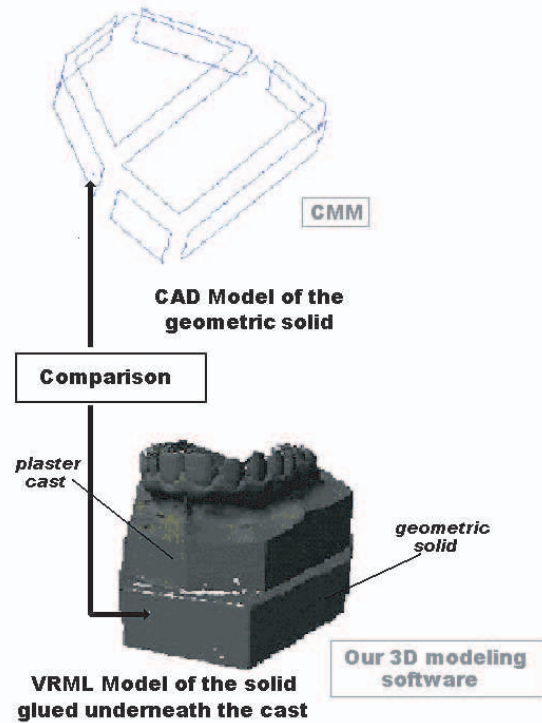


Figure 8. Comparison of the CMM based CAD model with the corresponding part of the 3D model of the augmented dental plaster cast.

4.2. Simulation analysis

In order to determine the contribution to error propagation due to the 3D modeling procedure of [1] alone, one would need to eliminate acquisition error. Such a possibility is clearly not at reach of any experimental setting but it can be pursued by way of simulation. Indeed, one can first take the 3D model of a plaster cast as ground truth. Then it may synthetically brake it into views very close to the 3D views obtained by way of actual acquisition and finally build a 3D model from the synthetically generated views by the 3D modeling procedure of [1] as pictorially indicated in Fig. 9. Since the acquisition error is intrinsically part of the ground truth as well as of the synthetically generated views, this procedure pictorially shown in Fig. 9 simply cancels it.

The global error obtained by reconstructing a 3D model from its 11 synthetically generated pieces and by considering it as ground truth has a standard deviation $\sigma = 0.1003mm$. The global error concerning only the cast's part, i.e. made from 6 3D views, rather the 11 3D views has instead $\sigma = 0.082mm$.

If we add to the synthetically generated views zero mean gaussian noise characterized by $\sigma = 0.04mm$, i.e., with a standard deviation comparable with that of the acquisition

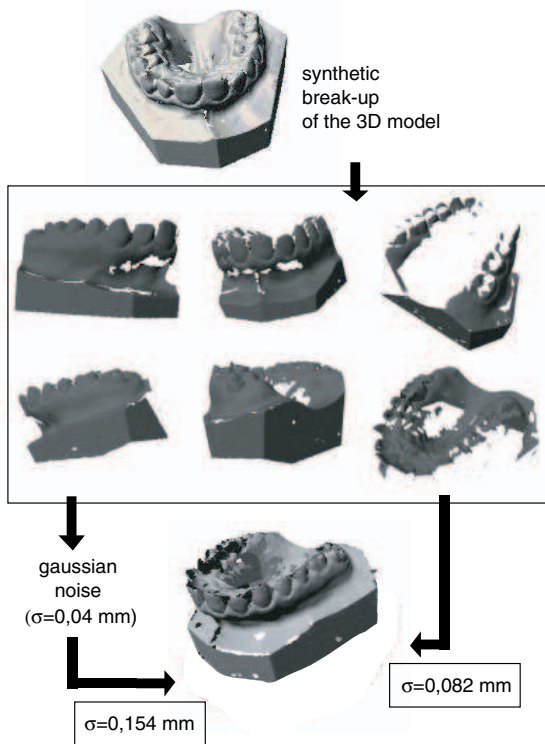


Figure 9. Synthetic break-up and reconstruction of a 3D model, with and without added gaussian noise.

error of our optical range-camera and build a 3D model by way of [1] from these data, we obtain $\sigma = 0.1957mm$. This value for the overall 3D surface's σ is not too far from $\sigma = 0.230mm$, the experimentally obtained value.

It is clear that modeling acquisition error as gaussian independent noise in each view is a convenient mathematical approximation, nevertheless it is remarkable how nicely in this case simulations based on this simple model match experimental data.

Therefore, based on the above observations, if we built a 3D model of the plaster cast alone by using the six needed views only, we find that the overall 3D surface's σ is $0.154mm$ as indicated in Fig. 9.

5. Conclusions

Procedures for automatic 3D modeling are highly desirable since, by waving from the need of human supervision, they can reduce 3D modeling costs, eliminate human errors and allow people without engineering training to make 3D models. In many applications, of which the medical field is an example, it is essential to know the accuracy of the 3D models, i.e., how close the points of the 3D models are to the true points of the objects they represent. As well known,

the errors of the 3D models are due to the acquisition or single view error and to the 3D modeling procedure. The latter can be ascribed to the various phases of the 3D modeling pipeline: pairwise registration, global registration, surface integration.

This work examines a task specific error analysis for plaster casts. We examined the acquisition errors, due to the measurement system, lighting conditions, workpiece and the operator, as well as the error due to an automatic procedure recently proposed for the 3D modeling of dental plaster casts [1].

From the metrological viewpoint, this work gives an example of how to carry a systematic experimental error analysis of a practical 3D modeling method for freeform surfaces, mainly through the comparison with the results of a CMM. It also shows that simple error propagation models can be rather useful for practical simulation purposes.

From a general viewpoint, it shows the quality of the automatic 3D modeling procedure of [1].

From an application viewpoint it shows the accuracy of 3D modeling dental plaster casts by current commercial range cameras and the automatic method of [1]. This information is rather valuable for dental doctors interested to replace the inventories of their dental plaster casts with virtual gypsosheques.

Let us finally add that we think that Markovian noise models should be more suited to represent 3D modeling error. We are currently investigating in this direction in the aim to effectively analyse the errors of 3D models made by a number of 3D views much larger than that of dental plaster casts.

Acknowledgments

We would like to acknowledge Prof. Giampiero Cordoli, Head of the Dental Clinic of the University of Padova for supplying us with the plaster casts and for his help in our research. We are also very grateful to Dr. Dennis Miotto of the Dental Clinic of the University of Padova for his assistance. Prof. Enrico Savio and Prof. Leonardo De Chiffre of DIMEG of University of Padova are acknowledged for their stimulating discussions and advices. We acknowledge Gabriele Bardella for running the experimental work and the simulations of this contribution. This work has been partially supported by the University of Padova under "Progetto di Ricerca di Ateneo CPDA024157-2002" and FIRB-PRIMO.

References

- [1] M. Andreetto, N. Brusco, and G. M. Cortelazzo, "Automatic 3D modeling of palatal plaster casts," in *Proc. 4th Int.Conf. on 3D Imaging and Modeling 3DIM, Banff, Canada, 2003*, pp. 132–138.

- [2] Wilhelm, R.G. Hocken, and R. Schwenke, "Task specific uncertainty in coordinate measurement," *Annals of the CIRP*, vol. 50, no. 2, pp. 553–563, 2001.
- [3] E. Savio, H. N. Hansen, and L. De Chiffre, "Approaches to the calibration of freeform artefacts on coordinate measuring machines," *Annals of the CIRP*, vol. 51, no. 1, pp. 433–436, 2002.
- [4] E. Trapet, E. Savio, and L. De Chiffre, "New advances in traceability of cmms for almost the entire range of industrial dimensional metrology needs," *Annals of the CIRP*, in press, 2004.
- [5] H. Rushmeier F. Bernardini, "The 3D Model Acquisition Pipeline," *Computer Graphics Forum*, vol. 21, no. 2, pp. 149–172, 2002.
- [6] A. Ashbrook, R. Fisher, C. Robertson, and N. Wergli, "Finding surface correspondence for object recognition and registration using pairwise geometric histograms," in *Proc. European Conference on Computer Vision*, 1998, vol. 1407, pp. 674–786.
- [7] C. Dorai, G. Wang, A. Jain, and C. Mercer, "Registration and integration of multiple object views for 3D model construction," *IEEE Transactions on Pattern Analysis and Machine Intelligence*, vol. 20, no. 1, pp. 83–89, November 1998.
- [8] K. Higuchi, M. Hebert, and K. Ikeuchi, "Building 3D models from unregistered range images," *Graphical Models and Image Proc.*, vol. 57, no. 4, pp. 315–333, 1995.
- [9] D. Huber and M. Hebert, "Fully automatic registration of multiple 3D data sets," *IEEE Workshop on Computer Vision Beyond the visible Spectrum*, pp. 433–449, December 2001.
- [10] D. Zhang and M. Hebert, "Harmonic maps and their applications in surface matching," in *Proc. of IEEE Conference on Computer Vision and Pattern Recognition (CVPR 99)*, November 1999, pp. 524–530.
- [11] A. E. Johnson, *Spin-Images: A Representation for 3-D Surface Matching*, Ph.D. thesis, Carnegie Mellon University, Pittsburgh, August 1997.
- [12] A. E. Johnson and M. Hebert, "Using Spin-Images for Efficient Multiple Model Recognition in Cluttered 3-D Scenes," *IEEE Transactions on Pattern Analysis and Machine Intelligence*, vol. 21, no. 5, pp. 433–449, 1999.
- [13] P. Krsek, T. Pajdla, V. Hlavac, and R. Martin, "Range image registration driven by hierarchy of surface differential features," in *Proc. 22nd Workshop of the Austrian Association for Pattern Recognition*, May 1998, pp. 175–183.
- [14] J. Vanden Wyngaerd and L. Van Gool, "Coarse registration of surface patches with local symmetries," in *Proc. European Conference on Computer Vision (ECCV'02)*, May 2002, vol. 2351, pp. 572–586.
- [15] J. Vanden Wyngaerd, L. Van Gool, R. Koch, and M. Proesmans, "Invariant-based registration of surface patches," in *Proc. International Conference on Computer Vision (ICCV'99)*, 1999, pp. 301–306.
- [16] L. Van Gool, D. Vandermeulen, G. Kalberer, T. Tuytelaars, and A. Zalesny, "Modeling shapes and textures from images: new frontiers," in *Proc. of 1st International Symposium on 3D Data Processing Visualization and Transmission (3DPVT2002)*, Padova, Italy, June 2002, pp. 286–294, IEEE Press.
- [17] G. Roth, "Registering two overlapping range images," in *Proceeding of the Second Intl. Conf. on 3D Digital Imaging and Modeling*, Ottawa, Canada, October 1999, pp. 191–200.
- [18] P. J. Besl and N. D. McKay, "A method for registration of 3D shapes," *IEEE Transactions on Pattern Analysis and Machine Intelligence*, vol. 14, no. 2, pp. 239–259, November 1992.
- [19] T. Jost and H. Hügli, "A Multi-Resolution Scheme ICP Algorithm for Fast Shape Registration," in *Proc. of 1st International Symposium on 3D Data Processing Visualization and Transmission (3DPVT2002)*, Padova, Italy, 2002, pp. 540–543, IEEE Press.
- [20] L. Lucchese, G. Doretto, and G. M. Cortelazzo, "A frequency domain technique for 3-D view registration," *IEEE Transactions on Pattern Analysis and Machine Intelligence*, vol. 24, no. 11, pp. 1468–1484, November 2002.
- [21] R. Bergevin, M. Soucy, H. Gagnon, and D. Laurendeau, "Towards a general multiview registration technique," *IEEE Transactions on Pattern Analysis and Machine Intelligence*, vol. 18, no. 5, pp. 540–547, 1996.
- [22] M. Wheeler, Y. Sato, and K. Ikeuchi, "Consensus surfaces for modeling 3d objects from multiple range images," in *Proc. of Sixth International Conference on Computer Vision*, 1998, pp. 917–924, IEEE.
- [23] *ISO 10360-2: 2001, Geometrical Product Specifications (GPS) - Acceptance test and reverification test for CMMs - Part 2: CMMs used for measuring size.*
- [24] I-DEAS, *Imageware Surfacer*, <http://www.team-eng.com/products/imageware/surfacer.html>.